Data Quality Report - 2019

Hyperspectral

NEODAAS

Updated on: October 17, 2019

Contents

1 Introduction

The NERC Earth Observation Data Acquisition and Analysis Service (NEODAAS) have processed hyperspectral data collected with NERC's Specim AISA Fenix instrument since 2014; formerly as the NERC Airborne Research Facility Data Analysis Node(NERC-ARF-DAN). The CCD array of the instrument was changed for a new one before the 2018 flight season.

The NERC Fenix instrument comprises two detectors covering the Visible to Near Infra-Red (VNIR) and Short Wave Infra-Red (SWIR) regions, giving a total spectral range of 380–2500 nm. It replaced previously operated sensors Eagle (400–970 nm) and Hawk (970–2500 nm) hyperspectral instruments. This data quality report describes issues for hyperspectral data acquired with the Fenix instrument that should be considered when further processing any NEODAAS datasets acquired from October 2018 including flights in 2019 until the start date listed in the succeeding data quality report.

This document may be updated over the course of the year, the latest version is available at:

https://nerc-arf-dan.pml.ac.uk/trac/wiki/Reports

2 Geo-referencing accuracy

NEODAAS currently delivers level 1b (calibrated at-sensor radiance) and level 3 data (mapped level 1b data). This offers users quick access to georeferenced data whilst maintaining the capability to operate on the original pre-gridded data and use a coordinate projection or datum of choice.

The quality of the geocorrection for each project is described in the documentation supplied with the delivery. Typically the geocorrection is of the order of a couple of metres, equating to approximately 1 pixel depending on flight altitude. High accuracy relies on an accurate Digital Surface Model (DSM). The freely available global ASTER digital elevation data are used during quality checks and an elevation model is supplied with the delivered mapped files. Accuracy may be improved by using a DSM derived from higher resolution data such as LiDAR. An indication of the average error between vector overlays is included in the delivery documentation where vector overlays or other ground truth information is available.

It may be possible to tune specific flight lines for higher accuracy and instructions can be provided on how to make your own alignments. If a higher accuracy is required, please contact us at: helpdesk@neodaas.ac.uk

3 Timing Errors

If the navigation data and scanline imagery are misaligned then it will manifest itself as a distortion in the geocorrected image. This misalignment is most often caused by an error in the timing, which means that the scanlines get syncronised to incorrect navigation (position and attitude). A timing error can range from a fraction of a second to tens or hundreds of seconds if the system crashes. An example is shown in Figure 1.

This issue was extensively investigated and fixed in 2016 for the NERC-ARF Fenix instrument. This fix also appears to apply to the loan instrument used in 2017. If any distortions are found in your data then please contact us at helpdesk@neodaas.ac.uk and we will investigate and correct (where possible).

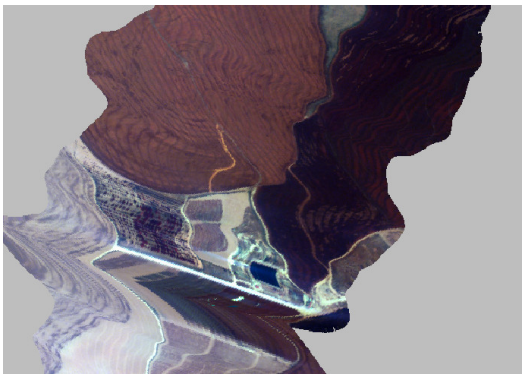

(a) *Timing error in a flightline.*

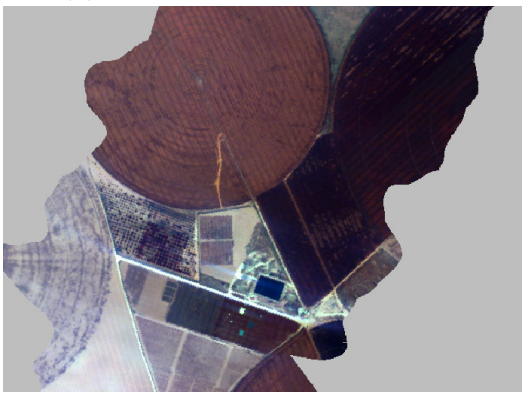

(b) *Corrected version of the above image (0.5 s timing difference).*

Figure 1: *Illustration of timing offset present in geo-referenced Fenix data.*

4 Sensor calibration

The Fenix sensor calibration is undertaken for every flight campaign in collaboration with the NERC Field Spectroscopy Facility to ensure spectral (wavelength) and radiometric accuracy. The calibration event in October 2018, undertaken at the British Antarctic Survey's facilities in Cambridge, covers all flights from that date onwards.

4.1 Wavelength calibration accuracy

Wavelength calibration is performed by collecting data from a range of spectral lamps. These lamps provide spectral emission features at known wavelengths that can be detected with the Fenix sensor. This procedure allows specific pixel numbers to be checked against known wavelengths. The lamps included in the calibration were: H, O, He, Kr, Xe, Ar, Ne, Hg-Ar and CO_2. The number of wavelengths tested was sufficient to be confident in the wavelength accuracy of the Fenix instrument. Differences from known spectral features versus their values measured by the Fenix can be found in Table 1.

The Full Width at Half Maximum (FWHM) values in these tables have been obtained by fitting Gaussian curves to the spectral features and then measuring the FWHM for the best-fitting curve. While this procedure gives a reasonable estimate of the FWHM values, some caution is recommended for applications relying on accurate FWHM values. Note that the FWHM as labelled in the data header (.hdr) files is the bandwidth of each band.

Spectral Line (nm)	**Measured Wavelength (nm)**	**FWHM (nm)**	**Error (nm)**	**Pass/Fail (<2nm Err.)**
435.8	435.99	2.62	-0.19	Pass
486.1	486.30	2.92	-0.20	Pass
546.1	546.05	2.63	0.05	Pass
578.1	578.01	4.18	0.09	Pass
594.4	594.06	2.17	0.34	Pass
656.3	656.09	3.33	0.21	Pass
667.6	667.68	3.38	-0.08	Pass
692.9	692.89	3.25	0.01	Pass
706.5	706.53	3.62	-0.03	Pass
717.4	717.61	3.15	-0.21	Pass
728.1	728.11	3.95	-0.01	Pass
738.4	738.36	3.38	0.04	Pass
750.9	750.78	3.76	0.12	Pass
763.5	763.48	3.50	0.02	Pass
785.5	785.42	3.22	0.08	Pass
801.1	801.06	3.47	0.04	Pass
811.1	811.06	3.63	0.04	Pass
823.2	823.12	3.28	0.04	Pass
849.5	849.53	3.00	-0.03	Pass
866.8	866.91	2.51	-0.11	Pass
877.6	877.74	2.97	-0.14	Pass
892.9	892.93	2.93	-0.03	Pass
912.3	912.34	2.83	-0.04	Pass
922.4	922.42	3.00	-0.02	Pass
965.8	965.75	2.61	0.05	Pass
	Mean	**3.17**	**±0.09**	
1083.0	1083.05	9.69	-0.05	Pass
1363.4	1362.16	17.78	1.26	Pass
1442.7	1441.02	15.49	1.66	Pass
1473.4	1474.25	10.84	-0.81	Pass
1816.7	1816.63	10.47	0.10	Pass
2058.7	2058.19	9.06	0.51	Pass
	Mean	**12.22**	**±0.73**	

Table 1: *Wavelength calibration offsets for the April 2018 calibration of the Fenix. Sections denote values for VNIR and SWIR detectors separately.*

4.2 Radiometric calibration accuracy

Radiometric calibration was undertaken on the Fenix instrument using an integrating sphere provided by the NERC Field Spectroscopy Facility. The sphere was calibrated in accordance with National Physics Laboratory Standards and a light source of known radiance was provided at each wavelength in use. This procedure allows a radiometric calibration curve to be obtained for the Fenix.

Radiometric calibration has been performed on the NERC Fenix on six separate occasions before 2018: December 2013, February 2014, February 2015 February 2016, April 2018 and October 2018. Due to a fault with the instrument prior to the 2017 season, a similar instrument was loaned from Specim for all 2017 campaigns. This instrument had an extra band, but otherwise data had similar characteristics and accuracy.

The NERC Fenix instrument was sent to the manufacturer (Specim) and a new CCD array was fitted in the instrument before the start of the 2018 flight season. The result is that the wavelength scale and radiometric coefficients differ slightly from previous years as expected but the wavelength scale is within same range and the sensor characteristics remain identical with the same number of bands than the original sensor.

Comparisons between the 2018 radiometric calibration carried out by the former NERC-ARF (now part of NEODAAS) and previous calibrations performed for the same instrument should therefore not be made because of the new CCD array fitted by the manufacturer on the Fenix instrument. A graph displaying the change between the two calibrations performed in April 2018 and October 2018 is shown in Figure 2. The regions displaying larger changes are mainly restricted to the edge of the detectors, where the bands have the lowest sensitivity and poorest performance. Please note that mean percentage differences are under 4% which indicates that the sensor was stable during this period of time with no signs of deterioration. The region around band 348 corresponds to the edge between the VNIR and SWIR detectors.

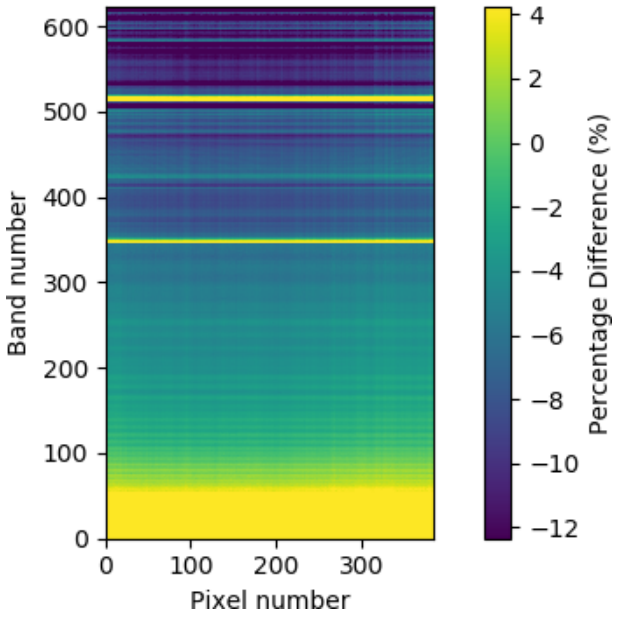

Figure 2: *Fenix calibration multiplier percentage differences between April 2018 and October 2018 calibrations. The region around band 348 corresponding to the edge between the VNIR and SWIR detectors and the edge of the detectors have a lower response and therefore we have the larger differences.*

5 Pixel Overflows

Hyperspectral instruments have a finite dynamic range and must be configured to capture data such that the received signal strength falls within this range. For example, if the area of interest is dark, then the instrument will be configured to capture as much low light as possible. Configuration of the Fenix instrument is set based on operator experience, prevailing conditions and the requested principal investigator's areas of importance. Inevitably some pixels are unexpectedly bright due to high responses recorded on the instrument, such as sunglint over water or reflected light from part of a cloud. These pixels may exceed the maximum capture level and 'overflow'. These pixels are not typically in areas of interest but should be accounted for when examining files. The accompanying mask file will contain an overflow flag value in the level 1 equivalent pixel. If you would prefer your actual level 1 files to be masked rather than use the separate mask file, please contact helpdesk@neodaas.ac.uk.

6 Bad CCD Pixels

The Fenix instrument has a varying number of pixels that provide inaccurate values, these are identified and flagged as 'bad pixels' during calibration. A list of known bad pixels has been included in the mask files supplied with processed data. Based on the type of Charge-Coupled Device camera used in the Fenix instrument $\sim$1 % of pixels (about 600) are expected to be bad. Bad pixels manifest in level 1 datasets as straight lines along the direction of flight and appear as undulating lines following the motion of the aircraft in level 3 data. An example is shown in Figure 3. Typically bad pixels will only affect a single wavelength band making detection difficult. A complete solution for identification and removal of bad pixels from the Fenix instrument was finalised in 2014 and is updated every year.

The final list of bad pixels uses six methods of detection that are executed on a set of test data. If a test fails for a particular pixel then that pixel will be flagged with that failure method. A flag is recorded for each test failed by that pixel, possibly resulting in multiple failure flags that are summed together. Masking of only certain bad pixel types is possible using the failure flags written to the mask file.

Figure 3: *Bad pixel on one Fenix band. On the left, bad pixel appears as a straight line in level 1 data; on the right, the same one is visible in level 3 as an undulating line.*

6.1 Detection method A - Constant input variable output (CIVO)

The CIVO method identifies pixels as bad pixels when they vary significantly given a constant light source as input. This is performed by considering the median raw value or Digital Number (DN) for the pixel over time, and testing individual epochs against a percentage threshold. If the value exceeds the threshold then the pixel is flagged as bad.

6.2 Detection method B - Constant input constant invalid output (CICO)

The CICO method identifies bad pixels when their response to a constant light greatly varies from the response of their spatial and/or spectral neighbours. As with the previous method the procedure is applied to raw values. To determine when a pixel's response varies it must be compared to its nearest neighbours.

To detect responses that differ significantly the mean and standard deviation of values are calculated for a moving window. These values are then used in the formula below.

$$B = \frac{\mu_c - \mu_{(s,b)}}{\sigma_{(s,b)}} \tag{1}$$

where μ_c is the mean of the CCD and $\mu_{(s,b)}$ and $\sigma_{(s,b)}$ are the mean and standard deviation over a window centred on sample s and band b. When B exceeds the threshold, the bad-counter for this pixel is incremented. Once the counter reaches the maximum allowed value, the pixel being tested is selected as bad.

6.3 Detection method C - Linear input non-linear output (LINO)

The LINO method takes the average DN for each pixel over time for multiple data captured at increasing integration times. Increasing integration time should have a direct linear sensor response for every pixel. Using regression over the average values versus integration time it is possible to get a measurement of linearity using the Pearson Correlation Coefficient (r). The closer r is to 1.0 the better the linear regression. The formula is given as:

$$r = \frac{\sum_{i=1}^{N} \left[(t_i - \bar{t})(d_i - \bar{d})\right]}{\sqrt{\sum_{i=1}^{N} \left[(t_i - \bar{t})^2\right] \sum_{i=1}^{N} \left[(d_i - \bar{d})^2\right]}} \tag{2}$$

where t is the integration time, d the mean DN for each pixel and $\bar{t}$ and $\bar{d}$ their means over the number of pixels tested (N). A pixel is flagged as bad if r is less than the threshold value.

6.4 Detection method D - Rapid saturation

The rapid saturation detection identifies a bad pixel if it is saturating more rapidly than its neighbours. This method works similarly to CICO to detect linear but invalid responses for different integration times. It compares the coefficients of the linear regression of mean pixel values versus integration times. As the previous method, a moving window of fixed spatial and spectral width will iterate over each pixel of each band. If the slope at the centre of the window being tested varies greatly in relation to its neighbours, then the pixel in that position will be flagged as a bad pixel. The function used to scan over each pixel is:

$$D = \frac{\mathrm{b}_c - \mu_{(s,b)}}{\sigma_{(s,b)}} \tag{3}$$

where, μ and σ are the mean and standard deviation and b_c is the slope of the CCD pixel given by a general regression:

$$Y = a + \mathrm{b}_c X \tag{4}$$

If D exceeds the threshold, then the pixel will be classified as bad.

6.5 Detection method E - Visual inspection

The visual inspection method consists of an extensive examination using in-house software. Pixels identified by an experienced analyst as giving erroneous results are selected as bad pixels. Erroneous results are identified by comparing those pixels with their neighbours. If a pixel is consistently brighter or darker than its closest pixels, it is marked as a bad pixel.

6.6 Detection method F - Detector sensitivity

The detector response is non-uniform across each of the bands. The lowest sensitivity is found in bands at the upper and lower limits of each detector. These bands have high calibration gains and noisy data may result in spikes in the radiometrically calibrated data. The normalised sensitivity (sensitivity for each band divided by maximum sensitivity for detector) is calculated, as shown in Figure 4. Bands with a sensitivity lower than a given threshold are marked as bad. Thresholds of <10 % and <30 % (or equivalently 0.1 and 0.3) are used to mask out bands in the VNIR and SWIR regions respectively. Separate thresholds are used for the VNIR and SWIR regions due to the different characteristics of each detector.

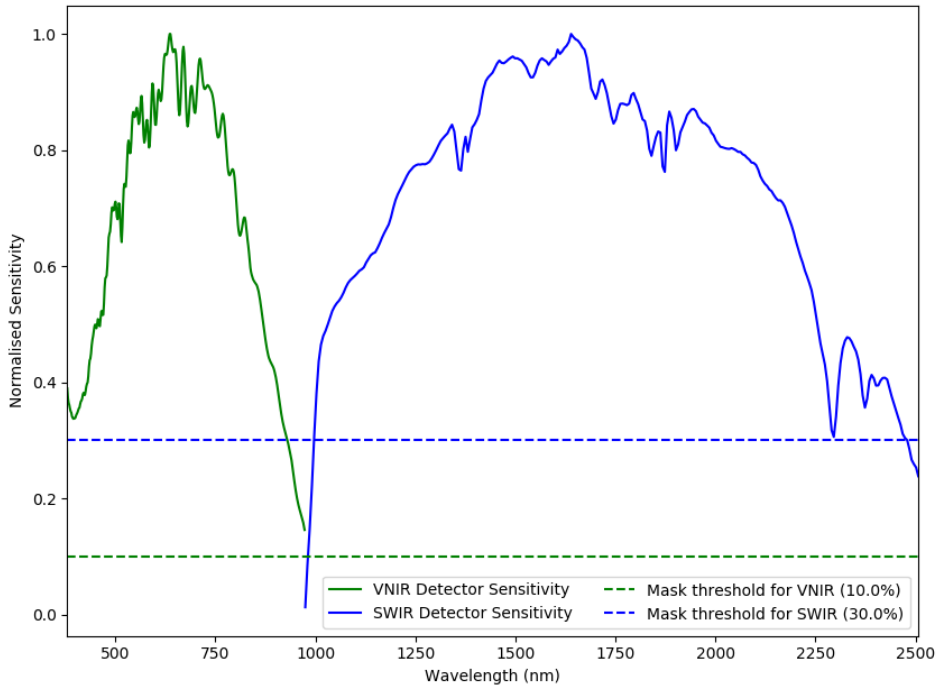

Figure 4: *Normalised sensitivity averaged over all pixels in the field of view of the VNIR and SWIR bands for Fenix detector.*